Information Capacity of Full-Body Movements

Antti Oulasvirta
Max Planck Institute for Informatics
Germany

Teemu Roos, Arttu Modig, Laura Leppänen
Helsinki Institute for Information Technology HIIT
University of Helsinki and Aalto University, Finland

ABSTRACT
We present a novel metric for information capacity of full-body movements. It accommodates HCI scenarios involving continuous movement of multiple limbs. Throughput is calculated as mutual information in repeated motor sequences. It is affected by the complexity of movements and the precision with which an actor reproduces them. Computation requires decorrelating co-dependencies of movement features (e.g., wrist and elbow) and temporal alignment of sequences. HCI researchers can use the metric as an analysis tool when designing and studying user interfaces.

Author Keywords
Information capacity; full-body movement; measurement; throughput; gesture-based interfaces; information theory

ACM Classification Keywords
H.5.m. Information interfaces and presentation (e.g., HCI): Miscellaneous.

INTRODUCTION
A fundamental problem for human–computer interaction (HCI) is to identify user interfaces that effectively map human movement to virtual movement. To assess joint human–computer performance, the "tempting but naïve" solution is to examine average speed and accuracy in a task [21]. This approach, however, overlooks the fact that data from easy and from difficult motor acts are incommensurable. Information theory has contributed to the measurement of user performance in HCI by providing a metric that collapses data on speed and accuracy into a single metric: *throughput* (bits/s, or bps) [7,12,13,21]. Throughput is often measured as statistical variability in *aimed movements* wherein the user brings an end-effector (pointer) on top of a spatially expanded target. *Information capacity* denotes the rate at which the user could have sent messages, given her speed and accuracy for given target properties. Selecting targets with the mouse, for instance, yields throughputs of 3.7–4.9 bps [17]. Although the metric has been contested, no better alternatives exist for comparing performance across tasks, conditions, and devices.

This paper extends the measurement of throughput from aimed movement to *full-body movement*—that is, multiple contributing limbs in continuous movement that does *not* need to be aimed at targets prescribed by an experimenter.

CHI 2013, April 27–May 2, 2013, Paris, France.

In so-called *configural* movements, the goal is to produce a shape or pattern in movement. This can be contrasted to aimed movements, wherein only the end point of movement counts. Examples would be drawing on a surface with multiple fingers, gesturing in the air to conduct a virtual orchestra, and dancing with motion sensors. In these examples, a user's ability to produce desired shapes reliably is more important than where in the space the movement ends.

Our method takes as input motion data with any number of movement features (observation points on the human body). It calculates throughput from *mutual information* of two or more deliberately repeated movement sequences. Our definition of mutual information captures the intuition that a skilled actor can produce complex (surprising) movements and reenact them precisely at will. Figure 1 illustrates *complexity* and *reproducibility* with the example of drawing a shape. For instance, linear motions with constant velocity, no matter how accurately repeated, are predictable and thus of low throughput. Analyzing precision in repeated efforts allows us to distinguish the controlled from uncontrolled aspects of movement. A newborn, for example, while able to produce complex-looking movements, does not have the capacity to reproduce them.

The metric is useful in HCI, because high throughputs potentially make more information available to an external observer such as a user interface—there are more "messages" the user could have sent by moving the body.

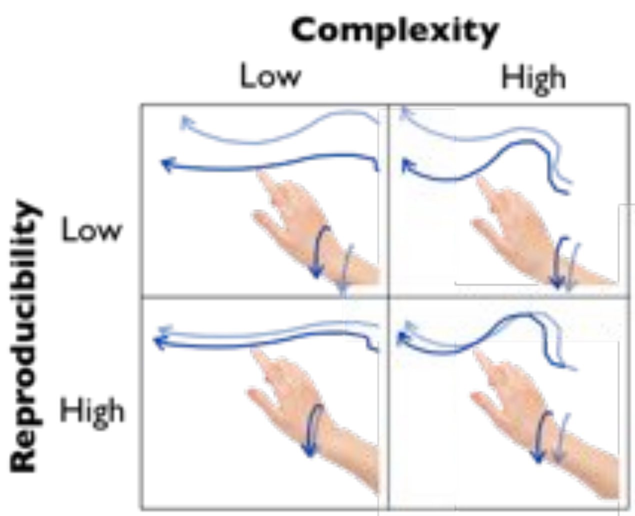

Figure 1. Information capacity is the mutual information of repeated movements (here: blue and light-blue trajectories), determined by their complexity and the precision of reproduction. Highly complex and precisely reenacted movements yield the highest throughputs.

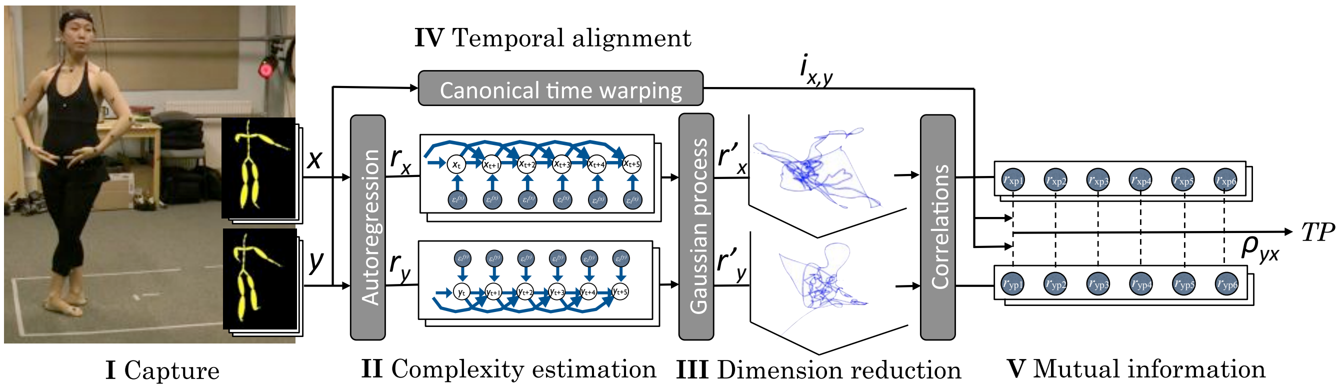

Figure 2. Overview of computation steps in calculating information capacity (TP) in full-body movement.

APPROACH

The concept of information capacity here follows the Gaussian channel interpretation of Paul Fitts [6,7,12] but applies it to mutual information I(x; y) in movement sequence x and its repetition y. I(x; y) denotes the reduction in bits in entropy of x when y is known. Since our I(x; y) excludes most of the uncontrolled movements and inaccuracies due to the actor's inability to repeat the movement precisely, it provides a measure of the *controlled* information in x and y. Computation is done in five steps (see Figure 2):

In **Step I: Motion Capture**, an actor is asked to carry out a movement and repeat it as precisely as possible. The motion of movement features is sampled. This procedure allows users to find natural ways to move—the only demand is that the same movement be repeated. In contrast, we believe that in some studies of aimed movements, constraining trajectories to end at experimenter-defined targets lowers throughputs. In **Step II: Complexity Estimation**, an autoregressive model is fitted to each movement feature. We take the residuals as an indicator of its complexity, or its "surprisingness." In **Step III: Dimension Reduction**, latent variable models are fitted to the residuals of x and y, reducing the co-dependencies among features. Non-linear dimension reduction is preferred in multi-feature motion data in order to avoid overestimation of throughput. In a violinist's movement, for example, it decreases correlation between the elbow and the wrist. In **Step IV: Temporal Alignment**, the best alignment of frames between x and y is identified. Temporal alignment is necessary in multi-feature data because the corresponding movement features of x and y may be differentially out of sync. In **Step V: Mutual Information**, I(x; y) is calculated by taking the frame-by-frame correlations of the model of x and y after dimension reduction. Throughput is now estimated as I(x; y) per second.

To assess the potential of the method for research and design in HCI, we report on three proof-of-concept studies. **Study I** studies information in a ballerina's performance, and **Study II** analyzes *trajectories* in aimed movement. **Study III** examines human factors in the bimanual gesturing scenario of the movie *Minority Report.*

We conclude by discussing limitations and use in HCI.

Background: Information in Aimed Movements

Because of space limitation, we refer the reader to existing reviews [7,13,21] and provide only the basics here. For *discrete aimed movements*, throughput *TP* is given by

$$TP = ID / MT \tag{1}$$

where *MT* is movement time and *ID* the index of difficulty. It is determined by the width of target *W* and its distance *D*:

$$ID = \log_2 (D / W + 1) \text{ [12], and} \tag{2a}$$

$$ID = \log_2 (2D / W) \text{ [6].} \tag{2b}$$

A variant generalizes a constant *TP* over a range of *D* and *W* conditions [21]. When *MT* obeys Fitts' law,

$$MT = a + b\, ID, \tag{3}$$

throughput is calculated as the slope of Fitts' model:

$$TP = 1 / b. \tag{4}$$

The benefit of using *TP* as an index of user performance is that it is found to be (relatively) robust to changes in the user's performance objective, or the speed–accuracy tradeoff. For example, trying to reach the target too rapidly results in lower accuracy, but *TP* remains in a constant range. A variant takes changes in performance objective into account by scaling *W* according to observed inaccuracies: The effective width is defined via the distribution of offsets from target center $W_e = 4.133\ \sigma$ [13,17]. Extensions of Fitts' law models to *continuous* aimed movements [1] covered only path width and length originally but were later extended to curvature [11]. However, to our understanding, these models have no interpretation in information theory.

Our metric shares with Fitts-*TP* the Gaussian channel interpretation of movement as a limited transmission channel [4]: *"information capacity is limited only by the amount of statistical variability, or noise, that is characteristic of repeated efforts to produce the same response"* [6: p. 262]. In our metric, changes in direction and velocity *during* movement determine complexity. As with the idea of W_e, variability in trajectories among the repeated efforts affects the total complexity of the repeated performance x and y. Our metric is also sensitive to changes in performance objectives (*Study II*).

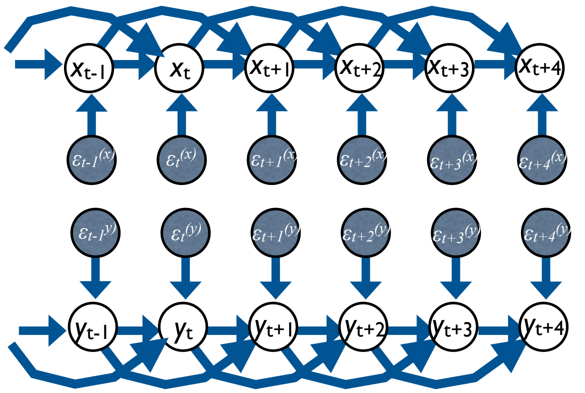

Figure 3. To estimate complexity, second-order autoregressive models are fitted to movements *x* (above) and *y* (bottom). Residuals ε_t expose the "innovativeness" of the trajectory.

COMPUTATION

We here present details for computing I(x; y).

Step I: Motion Capture

A pair of movement sequences is recorded in controlled conditions wherein an actor is asked to carry out a sequence (x) and repeat it as precisely as possible (y).

When performing y, the actor starts in the same initial position and posture. The repetition should take (about) as long as the original sequence. Multiple sequence pairs can be recorded, and throughput averaged over pairwise comparisons, but the unit of analysis is always a pair, and we focus here on that case. The administration of repetitions and the metric itself are agnostic of movement constraints: Trajectories in *aimed* movements can be analyzed, as we show in *Study III*. However, sometimes imposing constraints may lead to underestimation or overestimation of capacity, as in the case of sliding movements on a physical surface.

The collected data on x represent a movement sequence with a single *movement feature* or a set of them moving in time in a 2D or 3D coordinate system. Let $x = x_{-1},..., x_n$ denote a sequence where x_t gives the value of the measured feature at time t. Similarly, we denote by $y = y_{-1},..., y_n$ the repeated sequence of the same length. The multi-feature case is a vector of such sequences (see *Step III*).

Step II: Complexity Estimation

We let the complexity of a sequence be given by its entropy. We assume that both x and y follow *a second-order autoregressive* model (see Figure 3):

$$x_t = \beta_0 + \beta_1 x_{t-1} + \beta_2 x_{t-2} + \varepsilon_t^{(x)}, \quad (5)$$

$$y_t = \eta_0 + \eta_1 y_{t-1} + \eta_2 y_{t-2} + \varepsilon_t^{(y)}, \quad (6)$$

where β_0, β_1, β_2, and η_0, η_1, η_2 are real-valued parameters to be tuned via least squares. We start the sequence from x_{-1} instead of x_1 for notational convenience: the first two entries guarantee that an autoregressive model with a look-back (lag) of two steps can be fitted to exactly n data points (Figure 3). The benefit of a second-order model is its simplicity and interpretability: it captures the physical principle that once the movement vector (direction and velocity) is specified, constant movement contains no information. The errors (or "innovations") $\varepsilon^{(x)}$ and $\varepsilon^{(y)}$ are assumed to be zero mean Gaussian variates. Since the two sequences are supposed to be instances of the same movement pattern, they will typically be correlated. We denote the Pearson correlation coefficient of $\varepsilon^{(x)}$ and $\varepsilon^{(y)}$ by $\rho \in (-1,1)$. The innovations for different time frames $t \neq t'$ are assumed to be independent of each other. After parameter fitting, we obtain the *residuals*

$$r_t^{(x)} = x_t - \hat{x}_t = x_t - (\hat{\beta}_0 + \hat{\beta}_1 \hat{x}_{t-1} + \hat{\beta}_2 \hat{x}_{t-2}), \quad (7)$$

$$r_t^{(y)} = y_t - \hat{y}_t = y_t - (\hat{\eta}_0 + \hat{\eta}_1 \hat{y}_{t-1} + \hat{\eta}_2 \hat{y}_{t-2}), \quad (8)$$

where $\hat{x}_t$ and $\hat{y}_t$ denote the predictions obtained by plugging in least squares estimates $\hat{\beta}_0$, $\hat{\beta}_1$, $\hat{\beta}_2$, and $\hat{\eta}_0$, $\hat{\eta}_1$, $\hat{\eta}_2$, respectively. This formulation captures complexity as the shape of trajectory.

Step III: Dimension Reduction

In handling of p-dimensional sequences, $p > 1$, where each time frame x_t is composed of p measured movement features, $x_t = (x_t^{(1)},..., x_t^{(p)})$, it would be invalid simply to add up the information throughput of all of the features. For us to calculate the "genuine" capacity of the leg, any correlation in the movement of the knee and the calf must first be removed. We therefore perform dimension reduction.

Our preferred solution is *Gaussian Process Latent Variable Modeling* (GP-LVM)[16] administered separately on the residuals of x and y. GP-LVM models have been used to model human movement, such as walking [18]. In our experience, GP-LVM provides more effective dimension reduction than does *Principal Component Analysis* (PCA), which is limited to linear relationships. Using GP-LVM typically reduced *TP*s by a factor of 2–4 when compared to PCA. However, GP-LVM is (very) slow to compute. We have learned that, most of the time, dimension reduction with PCA preserves the order of *TP*s and can be used if absolute throughput values are unimportant.

For computation, we utilize *Fast GP-LVM* [10] to transform the two sequences and obtain two new time series, $r^{(x')}$ and $r^{(y')}$. Each frame in the new sequences represents a latent variable corresponding to a frame in the original sequence. Figure 4 shows a projection of a GP-LVM model with three latent dimensions.

For this step, the residuals of sequences are normalized such that each feature has mean zero and unit variance. Scaleinvariance is essential for the comparison of fine-grained and gross movements.

As we discuss in the next section, the number of latent variables (dimensions) in PCA/GP-LVM should be decided case by case by keeping reconstruction error at an acceptable level. In our studies, we have used *RSME* (root square mean error) as an indicator of reprojection error and used .05 as our criterion for an acceptable level.

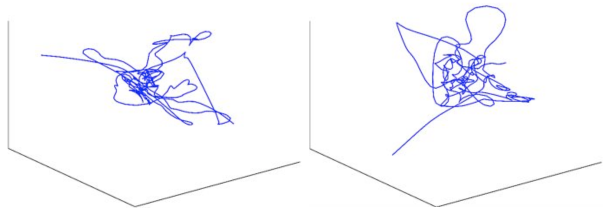

Figure 4. Two dimension-reduced dances: The plots are GP-LVM model manifolds with three latent dimensions.

Step IV: Temporal Alignment

A problem in predicting one motion sequence from another is possible temporal misalignment of the sequences and their features. Single-feature sequences can be aligned manually, but this is impossible with a large number of features. Even in carefully repeated movements, some features are more out of sync than others (e.g., the toe could lag behind the wrist). Hence, in prediction of the t^{th} frame of x, the most useful frame of sequence y may be not the t^{th} frame but the $(t+\delta)^{th}$ one, $\delta \neq 0$. Therefore, we must temporally align frames in x with frames in y.

Our solution is to align sequence pairs with *Canonical Time Warping* (CTW), a state-of- the-art technique for aligning sequences that describe human behavior [22]. CTW uses the more traditional *Dynamic Time Warping* [1] as an initial solution but improves it by adopting features from *Canonical Correlation Analysis*. The result is a pairwise alignment of x and y, $i_{x,y}$, such that each frame in x is matched to the most likely frame in y. To achieve this, CTW duplicates some of the frames in each sequence so as to "slow down" a sequence at suitable points. When measuring throughput, we skip duplicated frames in sequence x in order to avoid unnecessarily magnifying their impact. Hence, if frame t is duplicated in sequence x such that in the aligned sequence frames t and $t + 1$ are identical, we skip the $(t + 1)^{th}$ frame (of both x and y) when computing throughput. It is important to note also that in *Step II* we compute the residuals of both sequences from the *unaligned* sequences where there are no duplicate frames. Figure 5 shows an example in which two ballet sequences (*Study I*) have been aligned.

Step V: Mutual Information and Throughput

Under models (5) and (6), the differential entropy of each sequence can be estimated by plugging the residual variance into the familiar formula for the Gaussian entropy:

$$h(x) \approx \frac{n}{2}\log_2(2\pi e\hat{\sigma}_x^2), \quad h(y) \approx \frac{n}{2}\log_2(2\pi e\hat{\sigma}_y^2), \qquad (9)$$

where $\hat{\sigma}_x^2 = \sum_{t=1}^{n}(r_t^{(x)})^2/n$ is the residual variance of x.

The mutual information, which yields the reduction in bits in the entropy of one sequence when we are given the other, is now fully determined by the residuals and, in particular, their correlation ρ:

$$I(x;y) = -\frac{n}{2}\log_2(1-\rho^2)\,. \qquad (10)$$

However, since we do not in general know the true correlation coefficient, we need to estimate it from the data, which causes some statistical error. The statistical variation of the mutual information estimate obtained by plugging the empirical correlation coefficient into Eq. (10) can be characterized by means of results from classical likelihood ratio test theory [3,8]. In the case $\rho = 0$, the estimator asymptotically follows a χ^2 distribution scaled by a factor 0.5 or, equivalently, a Gamma distribution Γ ($k = 1 / 2$, $\theta = 1$), and in the case $\rho \neq 0$, its distribution is asymptotically Gaussian, centered at the true value of ρ. Hence, in the former case, the estimator has a positive asymptotic bias given by 0.5 times the mean of a χ^2 distributed random variable, $log_2(e)/2 \sim 0.731$ bits, where e denotes the Euler constant. Although we do not know in advance which of the two cases holds for each feature of the data sequences, we subtract the bias $log_2(e)/2$ from each feature, which gives a conservative estimate of $I(x; y)$. Consequently, we estimate

$$\hat{I}(x;y) = -\tfrac{n}{2}log_2\left(1-\hat{p}^2\right) - log_2(e)/2 \qquad (11)$$

where the last term is the bias correction.

The above method applies to unidimensional sequences. After the dimension reduction step, each movement sequence is represented as a sequence of (low-dimensional) feature vectors. In *Step V*, we handle each feature independently as described above and sum the obtained mutual information estimates to obtain the total throughput estimate $\hat{I}_{\text{tot}}$. We can then calculate *TP* in a multivariate sequence $\boldsymbol{x}$ conditioned on sequence $\boldsymbol{y}$ as $\hat{I}_{\text{tot}}(\boldsymbol{x};\boldsymbol{y})$ per second:

$$TP(x|y) = \frac{R\hat{I}_{tot}(x;y)}{n} = -\frac{R}{2}log_2\left(1-\hat{p}^2\right) - \frac{R}{2\,n}log_2(e), \qquad (12)$$

where R denotes the frame rate (frames per second).

Implementation

Computation takes, on average, about 2.5 seconds to run for two 111-feature ballet sequences of 1,100 frames, and about 7.5 s for another two dances approx. four times that length. With regard to the number of movement features, computation time scales linearly. However, times are longer with dimension reduction. While PCA adds only a few seconds, GP-LVM takes hours to days for such data. Below, we run some of our analyses with PCA. The caveat is that the absolute *TP*s values will be overestimated.

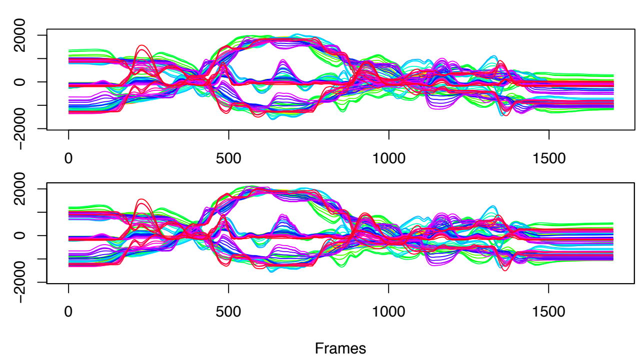

Figure 5. Two CTW-aligned sequences in the Ballet data. Each line is a one-dimensional movement feature. The y-axis shows deviation from starting position. The alignment of the first (top) and the second repetition (bottom) is nearly perfect.

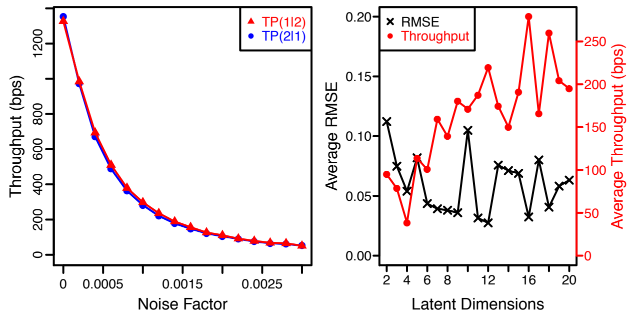

Figure 6. *Left*: The effect of noise in motion capture data on *TP* (PCA-based). *Right*: The effects of latent dimensions in GP-LVM on reprojection error (RMSE) and *TP*. Note that both the noise and the RMSE are relative to the standard deviation of the raw data.

TECHNICAL ASSESSMENT

We now report some technical properties of the metric.

Robustness to Noise in Motion Capture

Most studies of aimed movements have employed measurement instruments in which the level of noise is low. Noise is inevitable in motion capture data, however [20]. Ideally, the metric would tolerate a level of noise that does not obscure controlled aspects of movement. To understand the effect of noise, we added white noise with zero mean and variance to each feature to a dance from the Ballet data (*Study I*). Dimension reduction was done with PCA. Figure 6 (left) shows that even a small amount of additive white Gaussian noise—standard deviation of about 6×10^4 times the residual variance of each component—can halve the *TP*. In the movement of the dancer's toe, this corresponds to ~0.5 mm deviations. The result that *increasing* noise decreases *TP* and ultimately levels it is also a good sanity check: large noise makes the movements ridiculously complex, but because the two noise sequences are uncorrelated, the capacity decreases to zero.

Because of the sensitivity of the metric, we recommend smoothing data whenever noise may be a problem. We prefer cubic spline interpolation and Butterworth filtering, which are commonly used in analysis of motion data [20]. In our experience, this solution avoids rough smoothing that would decrease *TP*s.

Effects of Components in Dimension Reduction

The efficacy of dimension reduction is dependent on the number of components. Again, in studies of aimed movements, dimension reduction has not been an issue. In our case, an ideal metric decorrelates mutual information among movement features and achieves a tolerable level of error in modeling of the data with minimum components.

To chart the effect of component number, we manipulated the number of components in a GP-LVM model. As data we chose a segment from the dance *Adagio (temps lié)* in *Study I*. We charted *RSME* as an indicator of reprojection error and used .05 as our criterion for an acceptable level. Reprojected residuals differ from original data on average less than .05 units. Figure 6 (right) shows the result: component counts 6–9 are the first to reach the acceptable level. For component count 9, *TP* is around 160. Because the ideal number of latent dimensions in *Step III* varies from one dataset to another [18], we recommend choosing a model that reaches a tolerable level of reprojection error with the lowest number of components.

Effects of Temporal Alignment

An undesirable consequence of temporal alignment in *Step IV* is that we lose information about the temporal accuracy of the repetition. This is a drawback for activities wherein synchrony and timing are essential. To assess the impact of CTW, we compared *TP*s with and without it. In the Ballet data (*Study I*), we observed some increases in GP when CTW was performed. In the case of overly fast rapid caging of the hand (see below), however, CTW brought a sevenfold increase. We recommend analyzing *TP*s both with and without CTW when synchrony and timing are critical.

Static and Repetitive Movement

For a feasibility test, we checked whether very simple movements produce low *TP*s as they should. The following data (with repetitions) were collected via a *PhaseSpace* system with 12 *Impulse* cameras at 120 fps:

- Standing still (6001 frames)
- Balancing on one foot (1280 frames)
- Rapid caging of the palm (1698 frames)

In addition to optical markers for the full body, markers were placed on all fingers and both sides of the wrists. One of the co-authors served as the participant. We used CTW and GP-LVM with six latent dimensions.

As expected, balancing and standing produced virtually zero *TP*s, both *TP*s < 0.25 bps. As the person is standing still, residuals in complexity estimation are negligible. In balancing on one foot, swaying produces more complex movements in *Step II*, but because swaying is poorly matched from one sequence to another, even with CTW, *TP*s are negligible. This is not to say that balancing would not be motorically difficult, for it is [5]. And fitness games such as Nintendo Wii Fit Balance Board measure variation during balancing for score calculation. However, for an external observer such as an interface, it carries no information after observation of the initial pose.

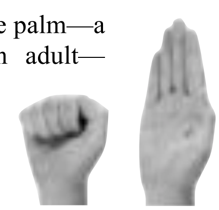

However, rapid, repeating caging of the palm—a motorically trivial movement for an adult—yielded a very high *TP* = 287.7 bps with GP. One drawback of the second-order autoregressive model is its short "memory": a human observer can easily detect repeats in a movement, but the model considers each repetition as surprising as the first instance. However, when CTW was removed, *TP* fell by a factor of 6.7, to 43 bps. The actor's high *TP* was achieved at the expense of accuracy in timing.

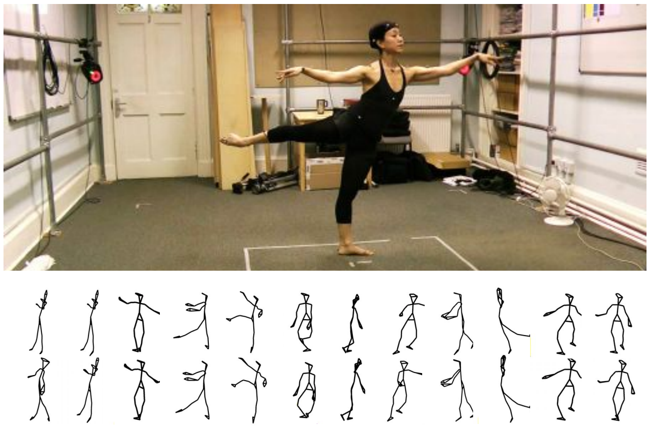

Figure 7. *Top*: Image from the recording of the Ballet dataset. *Bottom*: Snapshots of a sequence and its repetition.

STUDY I: BALLET

Computer vision and other sensors have enabled the mapping of almost any movement feature of a user's body to virtual movement; but how can we measure such performance and learn about it for design? In principle, a researcher could set up movement targets in a laboratory and chart the capacity of a user's limbs in *aimed* movements, one at a time and in combinations. This would be time-consuming, however, and would not capture information in trajectories or of the individual limbs.

Study I is a proof of concept demonstrating the suitability of our metric for analyzing very complex full-body performance. We study a skilled and highly overlearned multi-limb performance, ballet, as an analogue of the "highly overlearned" tapping movements in Fitts' studies [6]. We calculate throughput in a ballerina's movement to understand the metric in a situation wherein *all* movement features of the body are skillfully controlled for longer periods of time. We disregard the question of how actually to *map* physical movement to virtual movement in a real application and focus on how much information there is in theory.

Method

We recorded the performance of a teacher of classic and romantic ballet with several years of experience (Figure 7). Out of her vast repertoire, she was asked to select dances that would be fast, be complex and engage as many limbs as possible. The repetitions were to be as precise as possible, both temporally and spatially. These movements could be repeated as many times as desired until she was satisfied with the quality of the repetition. To assist her in quality-control, she was given the opportunity to see her performance from the recording device. Six sequences were eventually chosen (see Table 1).

The recordings were performed in a motion capture lab using *Vicon* with 12 *F40* cameras at 120 fps. For each frame, the data contain p = 111 features, corresponding to the 3D-coordinates of 37 markers. Butterworth smoothing was applied. For calculation of TP, we used PCA for all sequences with 90% of variance explained. PCA was carried out for the full sequence. We also calculated *TP* from the averages of GP-LVM performed on three segments of 500 frames. This analysis was carried out with and without CTW.

Findings

TPs for the dances are listed in Table 1. The table shows a range of 208 to 584 bps with GP. The worst-performing dance involved slow movement and stopping movement in static postures. The best-performing dance, by contrast, featured fast movements, circlings, and jumps.

Obviously, estimating *TP* from a single sequence yields a gross overestimation and the raw number per se is not informative. For instance, if the ballerina were to achieve 100 bps, she would move the 37 markers such that she sends one message out of 2^{100} alternative (distinguishable) messages per second! Achieving such rates in HCI would be impossible since the other implied dances would be required of the dancer. The metric can, however, be used for closer analysis of factors contributing to performance.

To understand the accuracy of timing and synchrony, we compared *TP*s with and without CTW (Table 1). Without CTW, the *TP*s are considerably reduced for some dances, but not for all. In contrast, the dance with the highest *TP* had almost no reduction when CTW was skipped. Figure 7 shows a matched sampling (from frames 0–3,960) of the dance and its repetition.

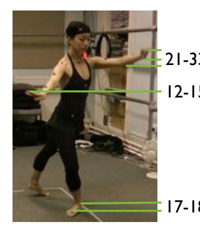

Furthermore, to understand which limbs are the best candidates for controlling an interface, we estimated limbs' contribution to the capacity. We averaged raw *TP*s per movement feature across the dances. As the adjacent figure shows, the two hands and the right foot had the largest throughputs, all above 12 bps. Markers for the torso, head, and distal parts of the feet had far lower values. This analysis reveals a laterality effect (left vs. right hand) and that torso and leg movements may be less well-rehearsed and important aspects of the teacher's dancing. An interface designer could use such information when mapping human movements to virtual controls.

Sequence	TP (raw)	TP (PCA)	TP (GP) CTW	No CTW
Tombé pas de bourrée, Italian fouetté, piqué turn, jeté en tournant	4092	1307	584	510
Adagio (passé devant développé, arabesque, écarté devant pas de bourré)	198	107	393	323
Petit jeté (glissade jeté, ballotté, ballon, entrechat, assemblé)	3335	755	308	283
Petit jeté (temps de cuisse, sissonne devant fermée, derrière fermée, sissonne ouvért pas de bourrée)	3013	764	238	191
Adagio (temps lié, arabesque, pas de bourrée, balancé)	1153	577	208	161
Grand jeté (battement développé, chassé, grande jeté développé, arabesque, fouetté sauté, jeté en tournant)	2654	698	267	141

Table 1. Throughputs in six sequences in the Ballet data

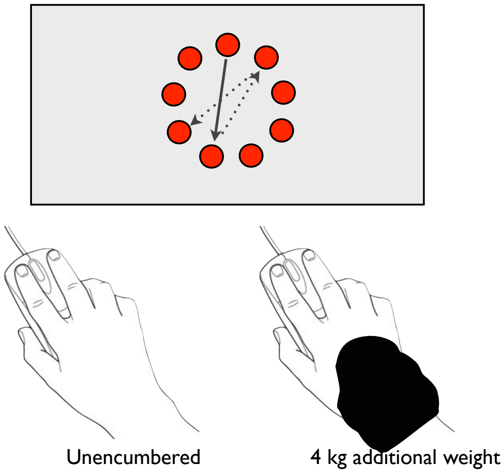

Figure 8. The setup of a cyclical tapping task done in two conditions: with and without an additional weight.

STUDY II: CYCLICAL TAPPING WITH MOUSE

Study II examines capacity in *aimed movements* in a cyclical selection task carried out with a mouse on a desktop PC (Figure 8, top). We chose to replicate a well-studied variant of the Fitts paradigm in order to compare our metric to the Fittsian metric. Although here not intending to "express information" when moving towards a target, the user spends most of the total time on the way. Our metric complements the Fittsian metric by showing that variability in trajectories is not always reducible to the Fittsian *TP*.

We predicted that our metric would show higher *TP*s in conditions wherein the approach trajectories can be kept close to each other. So with all else equal, decreasing *W* should increase *TP*. The shape of the curvature upon *turning* toward the next target should affect *TP* as well. A "spiky" turn would be surprising for the autoregressive model. To hamper such behaviors selectively, we added a condition with 4 kg wrist weight (see Figure 8).

Method

One of the authors carried out the experiment by using custom-made software that presented nine target circles on the monitor and recorded mouse clicks and movements at 96 Hz. Each trial consisted of clicking through the circle three times. After removal of the first tap of each trial, this yielded 26 clicks per trial. The *D* and *W* values were randomized from a range of $2.6 \leq ID \leq 6.1$, but the encumbrance condition (4 kg) was administered in only two *ID* conditions: $ID = 2.6$ and $ID = 6.1$, both with three repeats.

The subject was instructed to complete the task as quickly and accurately as possible. Plenty of practice was provided, both with and without the weight. The experiment was started only when performance with the weight had stabilized.

Findings

When effective width W_e is used as *W* in Eq. (2b) is used, *TP*s for the 0 kg and 4 kg conditions were 3.8 and 2.45 bps, respectively. This is in line with the range of *TP*s in previous studies [17]. As expected, the added weight had a decreasing effect (see [6]). The fits of our Fitts' law models were $R^2 = 0.90$ and $R^2 = 0.93$ for the two conditions, respectively (note, however, that using stimuli from only two *ID* conditions within the 4 kg condition improves the fit).

Our analysis reveals an interesting crossover when the novel *TP* metric is used. We compared trajectories from the conditions $ID = 2.6$ and $ID = 6.1$ between the 0 kg and 4 kg conditions and considered the complete movement trajectories from the each trial. We averaged the *TP*s obtained from pairwise comparisons. Dimension reduction and smoothing were unnecessary in this case.

The trajectories and *TP*s in each condition are presented in Figure 9. We made three observations: 1) In the unencumbered condition (0 kg), *TP*s are around 37 bps for both low and high *ID*s. Although *MT*s are higher in the high-*ID* condition, the trajectories are more closely "packed," which increases *TP*. 2) When the 4 kg wrist weight is added, *TP* in the low-*ID* condition falls to 24 bps. 3) Surprisingly, however, when $ID = 6.1$, *TP* with the 4 kg wrist weight is again 37 bps.

We observed that, with the added weight, the subject rotated his hand carefully in the high-*ID* condition before starting to move it toward the target. This is manifested in the closely aligned trajectories in Figure 9. Thereby the user compensated for the slower average movement velocity. In contrast, accurate premovement aiming was not necessary in the low-*ID* condition, since the targets were larger, and we saw more scattered trajectories and a reduction in *TP*.

We conclude that the two *TP* metrics can be used technically in the same experiment. We also conclude that a higher Fitts-*TP* in aimed movements does not imply a higher *TP* obtained from our metric.

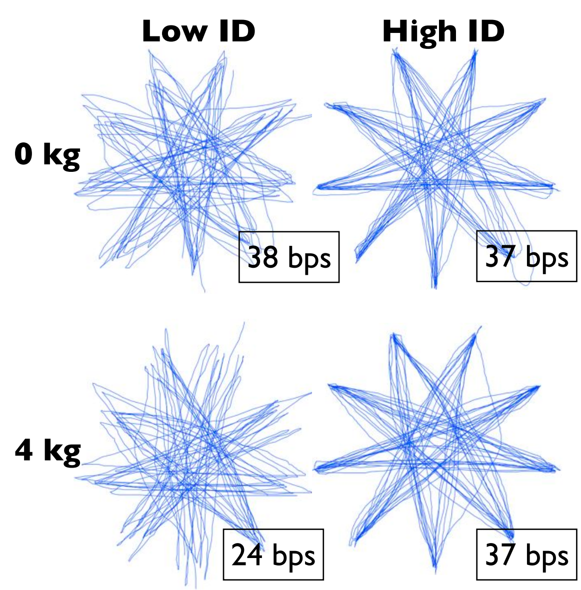

Figure 9. Movement trajectories (size normalized) and *TP*s in a cyclical tapping task with mouse.

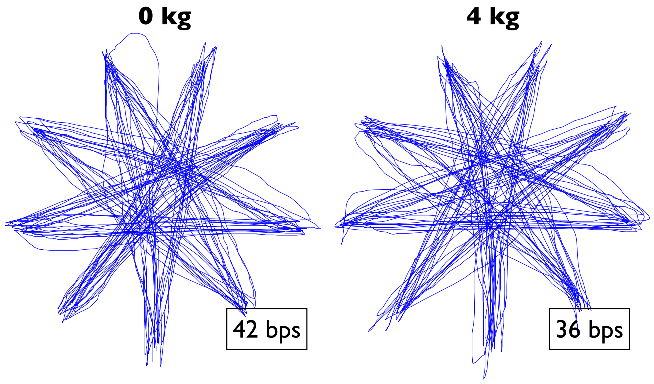

Figure 10. Movement trajectories and throughputs when a constant inter-click interval of 1000 ms was enforced (*ID* 4.1).

A Follow-up with Constant Time

We hypothesized that the surprising *benefit* of the wrist weight in the high-*ID* condition should disappear if the user is forced to make quicker movements. Rushing in the rotation-plus-aiming stage would result in less well-aligned trajectories. To test this hypothesis, the same subject carried out the task in a condition wherein *MT* was kept at a constant 1,000 ms with a metronome. The subject practiced performance before the experiment proper. Only one *ID* condition (4.1) was necessary for testing this hypothesis. After extensive practice, three trials were carried out per weight condition. The data were analyzed as previously.

As Figure 10 shows, the trajectories in the 0 kg condition (mean of *MT* 999.1 ms, *SD* 0.0793, target hitrate 95.0%) are much more closely aligned in space. In the 4 kg condition (mean of *MT* 1,005 ms, *SD* 0.0777, 89.6%), *TP* is markedly lower than in the 0 kg condition, as expected. With the increased tempo, it was indeed harder to perform accurate aiming in the premovement phase, which manifested itself in increased variability in trajectories.

STUDY III: BIMANUAL IN-AIR GESTURING

The problem of designing interfaces with full-body control is that the number of possible movements is too enormous to study empirically. One alternative would be to sample the space of possible movements aggressively [19] and average *TP*s. Another is to impose constraints in order to expose human factors relevant to interface design.

Our solution is to divide the interaction space into *movement conditions* and ask a user to produce an *overlearned motor act*, such as signing one's name, in each condition. The overlearned motor act is a surrogate for the complex movements that a user *could* produce with practice. The idea in such manipulations is that learned motor programs retain *some* invariance when transferred from a familiar context to another [15]. For example, one can sign one's name with the teeth or behind one's back. The effects of constraints such as position, rotation, or scale on *TP* show how robust the user's movements are to the conditions imposed by the interface. A usable interface sees uniformly high *TP*s across all commonly occurring conditions.

As a feasibility study we investigate the now-famous in-air gesturing scene in the movie *Minority Report* (Figure 11). The case is intriguing, because such interfaces are touted without regard for the fact that bimanual continuous control suffers from interference effects [14]. As the critical condition we study the *hand position*'s effect. Inspired by the movie, we assume a user gesturing with *both* hands raised to a space of 120° of the field of view. With this manipulation, we study whether user performance significantly changes if the hands are switched or operate at different distances from each other.

Method

In the experiment, the subject signs his name in the air with one hand and simultaneously makes another continuous movement, of the same duration, with the other hand (a G clef). The hands are interchangable. In our attempt to emulate the determination and skill of Captain John Anderton (played by Tom Cruise in the movie), our subject practiced the two movements, both in isolation and together, for three days before the experiment began. In the study, we divided the space in front of the standing subject into four segments, and asked him to perform the two movements in all combinations of segments such that the left hand is on the left side of the right hand. The dominant and the nondominant hand both performed the signature and the clef. In all, 12 trials were recorded, each with enough repetitions that the subject was satisfied with the precision of the repetition we included in our data. In a surprise test afterward, we asked the subject to change the clef to another gesture of similar complexity (the letter "g").

One author, a healthy male in his twenties, volunteered for the task. We used the *PhaseSpace* system with 12 *Impulse* cameras at 120 fps and a full-body tracking suit with additional markers on the fingers and wrists. For simplicity, we restrict the analysis to the two index fingers. Since we were interested in a comparison *within* the study, PCA was used for dimension reduction. Capacity is calculated as the average of the three best *TP*s achieved within a condition.

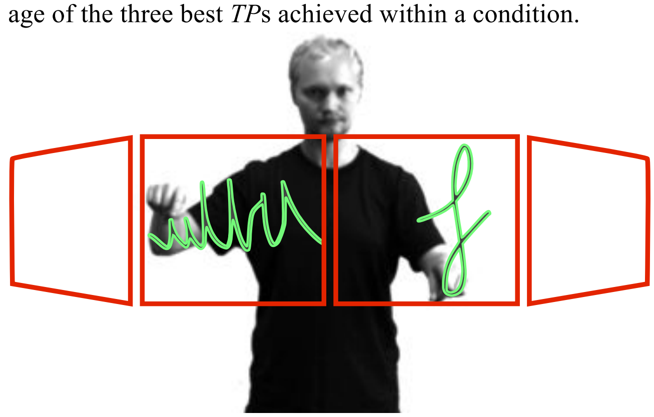

Figure 11.The *Minority Report* scenario is here studied in a task wherein a user produces bimanual gestures with two hands simultaneously. The segments of the movement space emulate those of an in-air UI.

Findings

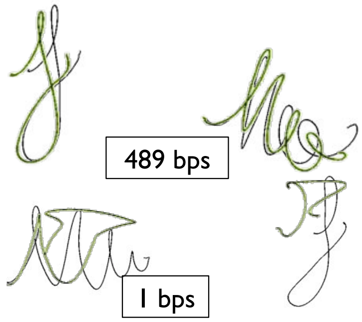

The adjacent figure shows as examples the best and the worst performances (repetitions superimposed on top of each other). Four observations were made. First, not surprisingly, throughputs (PCA) were higher for the dominant hand, with 217.8 bps vs. 199.7 bps for the dominant and the non-dominant hand, respectively. Second, the user could express genuine information with two-hand interaction: Throughput was 182.7 bps with dominant hand removed, 217.8 bps with non-dominant hand removed, and 322.1 bps with both hands. Thus, *bimanual* gesturing genuinely increased *TP* from that of single-handed gesturing. Third, changing the G-clef gesture to the previously unpracticed movement hampered bimanual capacity: the average throughput decreased by about 100 bps, from 322.1 to 220.5 bps. This *TP* is not far from the subject's singlehand performance. Fourth, the most surprising observation was that making the movements such that the hands are *close* to each other *lowered TP*. As shown by average *TP*s (PCA) in the three best repetitions per condition, the actor's performance was at its best with one segment (_) between the left and right hands:

L R	313.3 bps
L _ R	353.0 bps
L _ _ R	286.5 bps

A theory of bimanual distraction suggests that the distraction in the condition with the hands close to each other (here 61 cm apart) is due to perceptual distraction: *seeing* both hands moving distracts from their control [14]. When the hands are further apart (94 cm), there is less distraction. When the hands are very far apart (125 cm), control is again more difficult, perhaps for biomechanical reasons.

DISCUSSION

We have presented a novel metric for the information capacity of full-body movements. The new metric extends Fitts-*TP* metric by considering

- the shape of continous trajectory as the source of information instead of target width and distance and
- the accuracy of the reproduced movement as the source of noise instead of end-point variation.

The known extensions of Fitts' law from discrete to continuous movements are predictive models of *MT* (e.g., [1,11]) and do not carry an interpretation in information theory. Moreover, they are incapable of dealing with multi-feature arbitrary trajectories in 3D space. Our metric allows researchers to examine any scenario wherein users' motion can be represented as a sequence of vectors of movement features, from mouse movements to full-body motion. Naturally occurring movement can be analyzed, with the precondition that the data include matchable repetitions.

The metric is based on estimation of *mutual information* in repeated motor sequences. It should not be confused with the intrinsic *difficulty* of performing the movement nor with the motor system's capacity. In fact, neuromechanically simple mechanisms can produce high *TP*s, and some complex feats, such as balancing, have zero *TP*. Rather, the metric is best understood as an index of the information available to an external observer, as defined by the complexity and reproducibility of observed movements.

The new metric however, lacks one important feature of Fitts-*TP*: *interpolation*. Fitts-*TP* is relatively robust to changes in the target's *W* or *D*. This is possible because it accounts for discrete aimed movements that are produced by a simple agonist–antagonist neuromechanical pattern [5]. With more complex motor control, interpolation cannot be expected, because even slight changes in movement may involve entirely different control patterns.

The metric makes almost no assumption about the data, which makes it suitable for a wide range of uses. On the other hand, because of its generality, the *absolute TP* values are high when compared to the familiar range seen in aimed movements. This high range is expected, because the metric is based on high-frequency multivariate sampling of continuous movement but also because the model has no model of the performer, or the environment, as a prior. Even if the absolute values are high, however, we have shown that the metric responds as expected to conditions such as noise. To address the issue of high absolute values and improve the model, the most important goal for future work is to combine the now-separate steps of complexity estimation, temporal alignment, and dimension reduction in a single GP model. Further improvement can be achieved if complexity estimation is informed with a skeletal model of dimensions and movement ranges of bones and joints.

Applications

The metric can inform efforts in HCI where the expressiveness of continuous control is important. We foresee three use cases for the metric:

1. **Evaluation and comparison**: The metric can be used to study the motor capacity allowed by novel interface designs and to compare alternative solutions. Both tasks involve collecting movement data that span the space of possible movements. Because most movement spaces are too large to be exhausted empirically, complex overlearned patterns such as signatures (*Study III*) can be used to represent performance that users could attain with practice. Comparative studies should target obtaining a large number of comparable complex movements produced with each user interface.
2. **Analysis**: We showed that the metric is sensitive to some well-known effects in motor control, such as that of laterality (*Study III*), encumbered movement (*Study II*), change in performance objective (*Study II*), and

perceptual distraction of bimanual control (*Study III*). The metric can also be used to analyze the contributions of different limbs in users' continuous full-body movements (*Study I*) and to expose performance-affecting factors (*Study III*). Temporal alignment (CTW) can be dropped for estimation of the accuracy of timing and synchrony. The metric can also expose patterns in trajectories of *aimed* movements (*Study II*).

3. **Exploration**: Because the metric allows studying throughput independent of a intermediary device or target conditions, it can be used to explore potentials for user interfaces. For example, if there are multiple ideas on how a game could be controlled, they can be compared through asking users to produce the same movement sequences within each condition.

Unlike with Fitts-*TP*, calculation of the novel metric is computationally intensive, particularly if GP-LVM is used. Intensity is unavoidable, because the metric must account for multiple movement features moving over time. Moreover, it must addess three issues inherent to throughput calculation in multi-feature data: estimating the complexity of a trajectory, decorrelating interrelated features, and aligning sequences in time. Future work can explore efficient simplifications to this pipeline.

To help practitioners apply the metric, we provide a Web service. After sending movement data, the user chooses parameters for the five steps in the computation. The output contains an overall *TP,* a breakdown by movement feature, and the optio of analyzing different time segments. We provide a converter from angular representation (angles of joints) to the coordinate system (*x*, *y*, *z* position).

ACKNOWLEDGEMENTS

This work has been funded by the Academy of Finland (Starting Grant Booster, the Finnish Centre of Excellence in Computational Inference Research COIN 251170, MODEST), the Max Planck Center for Visual Computing and Communication (MPC-VCC), EIT ICT Labs, and the Emil Aaltonen Foundation. We thank Rod Murray-Smith, Heiko Drewes, John Williamson, Per Ola Kristensson, Antti Honkela, Miikka Miettinen, David MacKay, and Scott Klemmer for helpful comments. Also, we are indebted to Frank E. Pollick, Walter Boot, Christian Theobalt, and Carsten Stoll for sharing equipment and data, and to Naree Vachananda for the beautiful ballet. Code, data, and the service are available through our project page.

REFERENCES

1. Accot, J., and Zhai, S. Performance evaluation of input devices in trajectory-based tasks: an application of the steering law. *Proc. CHI'99*, ACM Press (1999), pp. 466-472.
2. Berndt, D., and Clifford, J. Using dynamic time warping to find patterns in time series. In *AAAI-94 workshop on knowledge discovery in databases,* vol. 2 (1994).
3. Brillinger, D.R. Some data analyses using mutual information. *Brazilian J. Probability and Statistics 18*, (2004), 163-183.
4. Cover, T., Thomas, J., and Wiley, J. *Elements of Information Theory*. Wiley Online Library, 1991.
5. Enoka, R. *Neuromechanics of human movement.* Human Kinetics Publishers, 2008.
6. Fitts, P. The information capacity of the human motor system in controlling the amplitude of movement. *Journal of Experimental Psychology 47,* 6 (1954), 381.
7. Fitts, P., and Posner, M. *Human Performance*. Brooks/Cole, Belmont, CA, 1967.
8. Kendall, M.G., and Stuart, A. *The Advanced Theory of Statistics*, Hafner, New York, 1968.
9. Lashley, K. An examination of the continuity theory as applied to discriminative learning. *Journal of General Psychology* (1942).
10. Lawrence, N. Probabilistic non-linear principal component analysis with gaussian process latent variable models. *The Journal of Machine Learning Research 6* (2005), 1783–1816.
11. Liu, L., and van Liere, R. The effect of varying path properties in path steering. *Proc. EGVE/EuroVR/VEC*, Eurographics Assoc. (2010), pp. 9-16
12. MacKenzie, I. A note on the information-theoretic basis for Fitts' law. *Journal of Motor Behavior 21,* 3 (1989), 323–330.
13. MacKenzie, I. Fitts' law as a research and design tool in human-computer interaction. *Human-computer interaction 7,* 1 (1992), 91–139.
14. Mechsner, F., Kerzel, D., Knoblich, G., and Prinz, W. Perceptual basis of bimanual coordination. *Nature 414,* 6859 (2001), 69–72.
15. Pew, R. Performance of human operators in a three-state relay control system with velocity-augmented displays. *IEEE Transactions on Human Factors in Electronics,* 2 (1966).
16. Rasmussen, C., and Williams, C. *Gaussian Processes for Machine Learning*. MIT Press, Cambridge, 2006.
17. Soukoreff, R., and MacKenzie, I. Towards a standard for pointing device evaluation: Perspectives on 27 years of Fitts' law research in HCI. *International Journal of Human-Computer Studies 61,* 6 (2004), 751–789.
18. Wang, J., Fleet, D., and Hertzmann, A. Gaussian process dynamical models for human motion. *IEEE TPAMI 30,* 2 (2008), 283–298.
19. Williamson, J., and Murray-Smith, R. Rewarding the original: explorations in joint user-sensor motion spaces. *Proc. CHI'12*, ACM Press (2012), pp. 1717-1726.
20. Winter, D., Sidwall, H., and Hobson, D. Measurement and reduction of noise in kinematics of locomotion. *Journal of biomechanics 7,* 2 (1974), 157–159.
21. Zhai, S. Characterizing computer input with Fitts' law parameters: The information and non-information aspects of pointing. *IJHCS 61,* 6 (2004), 791–809.
22. Zhou, F., and De la Torre, F. Canonical time warping for alignment of human behavior. *Proc. NIPS,* (2009), 1–9.